

## Extremely high-power tongue projection in plethodontid salamanders

Stephen M. Deban<sup>1,\*</sup>, James C. O'Reilly<sup>2</sup>, Ursula Dicke<sup>3</sup> and Johan L. van Leeuwen<sup>4</sup>

<sup>1</sup>Department of Biology, 4202 East Fowler Avenue, SCA 110, University of South Florida, Tampa, FL 33620, USA, <sup>2</sup>Department of Organismal Biology and Anatomy, University of Chicago, 1027 E. 57th Street, Chicago, IL 60637, USA, <sup>3</sup>Brain Research Institute, University of Bremen, 28334 Bremen, Germany and <sup>4</sup>Experimental Zoology Group, Wageningen Institute of Animal Sciences (WIAS), Wageningen University, Marijkeweg 40, 6709 PG Wageningen, The Netherlands

\*Author for correspondence (e-mail: sdeban@cas.usf.edu)

Accepted 22 November 2006

### Summary

Many plethodontid salamanders project their tongues ballistically at high speed and for relatively great distances. Capturing evasive prey relies on the tongue reaching the target in minimum time, therefore it is expected that power production, or the rate of energy release, is maximized during tongue launch. We examined the dynamics of tongue projection in three genera of plethodontids (*Bolitoglossa*, *Hydromantes* and *Eurycea*), representing three independent evolutionary transitions to ballistic tongue projection, by using a combination of high speed imaging, kinematic and inverse dynamics analyses and electromyographic recordings from the tongue projector muscle. All three taxa require high-power output of the paired tongue projector muscles to produce the observed kinematics. Required power output peaks in *Bolitoglossa* at values that exceed the greatest maximum

instantaneous power output of vertebrate muscle that has been reported by more than an order of magnitude. The high-power requirements are likely produced through the elastic storage and recovery of muscular kinetic energy. Tongue projector muscle activity precedes the departure of the tongue from the mouth by an average of 117 ms in *Bolitoglossa*, sufficient time to load the collagenous aponeuroses within the projector muscle with potential energy that is subsequently released at a faster rate during tongue launch.

Supplementary material available online at  
<http://jeb.biologists.org/cgi/content/full/210/4/655/DC1>

Key words: elastic storage, amphibian, feeding, inverse dynamics, kinematics, muscle.

### Introduction

Ballistic movements such as throwing and jumping maximize performance in distance, height or velocity by maximizing power output, or the rate of increase of kinetic energy. Maximizing power is necessary because the projectile – a limb or the entire body – must achieve the highest possible kinetic energy and velocity within a limited excursion (Alexander, 1968; Olson and Marsh, 1998; Alexander, 2002).

In musculoskeletal systems that are capable of rapid movements, the power that is required to produce the observed velocity and acceleration often exceeds the peak instantaneous power output capability of vertebrate muscle, which has been measured at 1121 W kg<sup>-1</sup> (in quail pectoralis) (Askew and Marsh, 2001). In systems that have power requirements in excess of what muscle can produce directly, muscles are still performing the work required for the movement. However, the rate of performing the work is decoupled from the rate at which it is transmitted to the environment. This decoupling typically results in greater rates of energy release (i.e. higher power) and

relies on the presence of elastic structures, such as tendons and aponeuroses, which lie between the muscle and the point of interaction with the environment. These structures are deformed by muscle forces and subsequently recoil to perform the same work much more quickly than the muscle (Alexander, 2002).

One such ballistic system in which 'elastic power enhancement' has been implicated is jumping in the bushbaby *Galago senegalensis*. The vastus muscle complex of these mammals generates up to 2350 W kg<sup>-1</sup> (Bennet-Clark, 1976), and is hypothesized to store energy in aponeuroses, energy that is released during the latter part of the push-off (Aerts, 1998). Another ballistic system that is particularly relevant to the current study is tongue projection in the chameleon, in which the required muscle-mass-specific power output reaches 3168 W kg<sup>-1</sup>. It is thought that this power output is achieved by the deformation and recoil of nested collagenous sheaths within the tongue muscle (de Groot and van Leeuwen, 2004).

Like chameleons, some plethodontid salamanders are

capable of ballistic tongue projection over great distances; the tongue can be projected up to 80% of body length in less than 20 ms. The distance of tongue projection, combined with the short duration over which projection occurs, suggests that tongue projection is a high-power behavior, and that elastic power enhancement may occur (Deban et al., 1997; Deban and Dicke, 1999; Deban and Dicke, 2004).

Using a combination of kinematic analyses, inverse dynamics and electromyographic recordings from the tongue projector muscles, we investigated the mechanics of tongue projection in representatives of each the three clades of plethodontid salamanders that have independently evolved ballistic tongue projection. Goals of this study were to (1) determine the work and power output of ballistic tongue projection in each of the three clades with ballistic projection; (2) determine if sufficient muscle is available, in each clade, to directly produce the observed power, or if an elastic power enhancement system must be operating; and (3) determine whether the timing of projector muscle activity relative to tongue movements is consistent with direct muscle action or with the alternative mechanism of elastic power enhancement.

### Materials and methods

Salamanders used in this study were wild-born individuals housed in aquaria or plastic containers with a substrate of moist paper towels at 22–24°C. They were maintained on a diet of crickets, houseflies, waxworms, flour beetles and termites.

Salamanders were imaged at 22–24°C in lateral or dorsal view while feeding on crickets, termites, waxworms and flour beetles. Images were obtained from one individual each of *Hydromantes platycephalus* (62 mm snout–vent length, *SVL*) and *H. imperialis* (70 mm *SVL*), two individuals of *H. genei* (63 and 67 mm *SVL*), seven individuals of *Bolitoglossa dofleini* (70–125 mm *SVL*), one *Eurycea guttolineata* (49 mm *SVL*) and two *Eurycea wilderae* (30 and 32 mm *SVL*). The cave salamanders (*H. imperialis* and *H. genei*) fed more readily in low light, hence they were imaged at 1000, 1600 or 2000 Hz with a Redlake MotionPro (Tucson, AZ, USA) using a single fiber optic microscope lamp 1 m from the subject combined with a retro-reflective background to yield a sharp silhouette of the salamander (Fig. 1). The *H. platycephalus* were recorded with a NAC (Simi Valley, CA, USA) HCS1000 and the *Bolitoglossa* and *Eurycea* were recorded using a Redlake MotionMeter, all at 1000 Hz with synchronized stroboscopic illumination, yielding greyscale video images of the salamanders (Figs 2, 3). A calibration grid of 1 cm squares was imaged separately, in the same plane as the animal, for each set of trials to eliminate parallax problems.

A total of 96 feedings were recorded on video, from which kinematic data were obtained. Of these, accompanying EMG data were collected from 25 feedings in three individuals of *Bolitoglossa dofleini* (95–105 mm *SVL*) (11, 10 and 4 feedings; one of the 25 feedings had no video data). Seven individuals of *Bolitoglossa dofleini* fed a total of 58 times (25, 11, 10, 4, 4, 2 and 2), two individuals of *Eurycea wilderae* fed 13 times

(10 and 3), one *Eurycea guttolineata* fed seven times, one *Hydromantes genei* fed five times, one *Hydromantes imperialis* fed twice, and one *Hydromantes platycephalus* fed 11 times. All methods in this study were approved by all appropriate Institutional Animal Care and Use Committees.

### Kinematic analysis

The *x,y* coordinates of the tongue tip were recorded for each frame of the video sequences (using NIH Image running on a Macintosh computer), starting with the first appearance of the tongue at the mouth and ending with the withdrawal of the tongue pad into the mouth at the end of tongue retraction (see supplementary material, Movies 1–3). Maximum tongue reach was calculated as the maximum excursion of the tongue tip (i.e. rostral tip of tongue skeleton) from its initial position. Relative maximum tongue reach was expressed as a percentage of *SVL*.

The movement of the tongue tip was used in the dynamics calculations because the tongue tip was visible throughout projection, and because it was deemed an acceptable surrogate for the movement of the center of mass of the projected tongue. Two sources of error could arise from using the tongue tip as a surrogate for center of mass, both involving potential shifting of the center of mass relative to the tongue tip: caudal shifting of the tongue pad on the tongue skeleton during tongue acceleration, and folding of the tongue skeleton. We examined preserved specimens of all genera and compared them to the feeding images and conclude that these sources of error are slight. The tongue pad changes length by no more than 6% during the period of maximum acceleration (in the 21 feeding sequences in which it was measured in *Hydromantes*, *Eurycea* and *Bolitoglossa*), and the tongue skeleton is folded (i.e. ceratobranchial, epibranchial and basibranchial are nearly collinear) when the tongue tip reaches the distance from the mouth at which maximum acceleration is achieved [a thorough discussion of tongue skeleton folding is published elsewhere (Lombard and Wake, 1976; Lombard and Wake, 1977)].

Instantaneous velocity, acceleration and mass-specific power of the projected tongue were calculated from the position data. A quintic spline was fitted to the raw position data using QuickSAND (Walker, 1997), because this technique is unlikely to overestimate velocities and accelerations (Walker, 1998). The interpolation function was used and the program yielded smoothed position, velocity and acceleration values at a final rate of 5000 Hz, regardless of the rate of the original data (1000–2000 Hz). The smoothing parameter, *P*, for the quintic spline was adjusted separately for each feeding trial so that secondary oscillations were removed from the acceleration trace. This required greater smoothing than necessary to remove these oscillations from the position and velocity data, and resulted in more conservative estimates of acceleration and velocity. Instantaneous mass-specific power of the tongue was calculated by multiplying the instantaneous velocity by the corresponding instantaneous acceleration.

The observed tongue-mass-specific power was then converted to required muscle-mass-specific power (i.e. the specific power that the muscles must produce to explain the

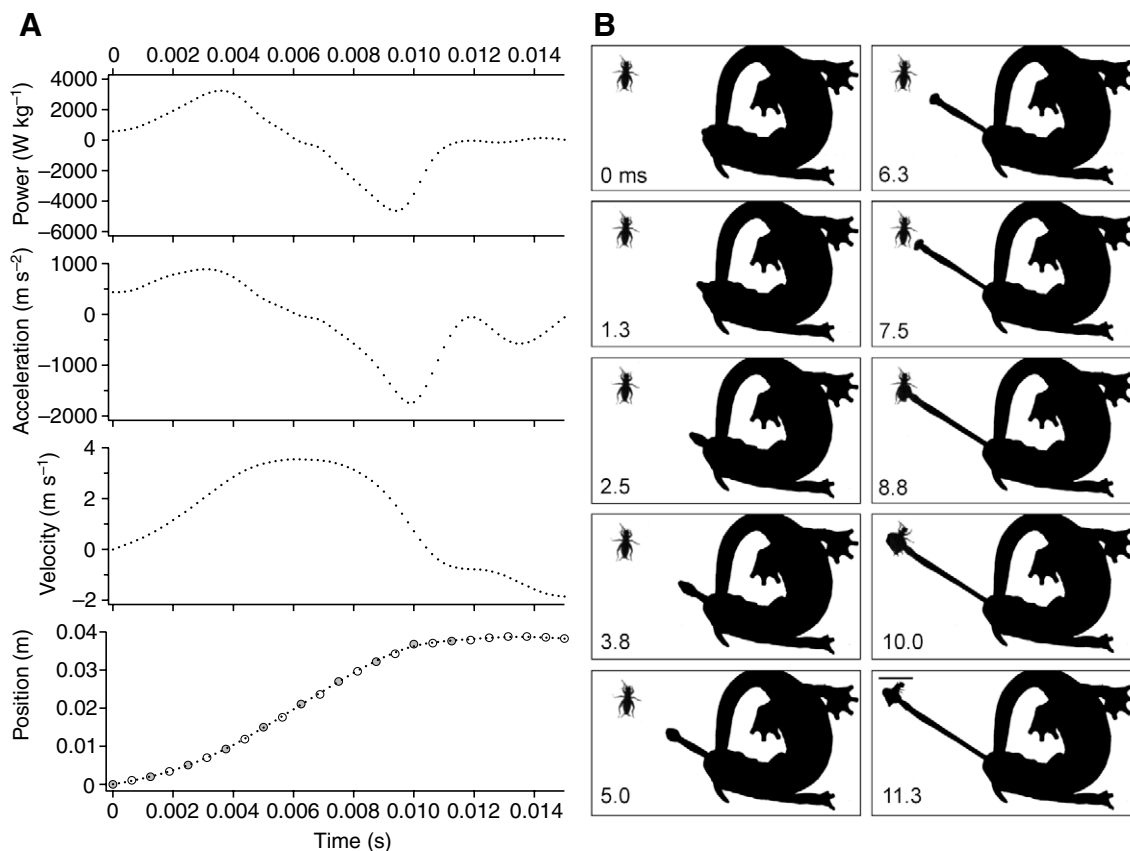


Fig. 1. (A) Kinematic profiles from a representative feeding in *Hydromantes genei* showing required instantaneous muscle-mass-specific power versus time in the upper trace, and instantaneous acceleration, velocity and smoothed and interpolated position versus time in the lower traces. Open circles in the position trace indicate raw position data, and the filled circles correspond to the video frames shown in B. (B) Image sequence of the same feeding from which the kinematics in A were derived. Scale bar, 1 cm; times (ms) are from the start of tongue projection. Note the long tongue reach and the peak required power output of over 3000 W kg<sup>-1</sup>.

observed kinematics). The masses of the tongue and the paired tongue projector muscles (left and right sides summed) were measured in preserved and fresh specimens of *Hydromantes imperialis*, *Bolitoglossa dofleini* and *Eurycea guttolineata*. Tongue mass included the combined mass of the tongue skeleton, the tongue pad, and a portion of the retractor muscle (m. rectus cervicis) equal to the length of the tongue skeleton. Preserved tongues were rehydrated in amphibians Ringer solution prior to weighing. Muscle-mass-specific power output values that would be required by the projector muscles (required specific power) were computed by multiplying the observed specific power values of the projected tongue by the average ratio of tongue mass to projector muscle mass (*TIM* ratio), which was 0.79 for *Bolitoglossa*, 1.04 for *Hydromantes*, and 1.29 for *Eurycea*.

Mass-specific work of the projector muscles (J kg<sup>-1</sup>) was calculated by taking the area under the positive portion of the mass-specific power–time curve. The required mass-specific power and mass-specific work values for the muscles computed are underestimates, not only because of smoothing of the position data but also because the frictional forces and other drag forces that resist tongue projection are assumed to be zero

in this analysis. In the animal, some energy is expended to overcome these forces.

Times of maximum tongue reach, maximum velocity, maximum acceleration and maximum power were calculated with respect to the time ( $t=0$ ) at which tongue instantaneous power reached 1% of the maximum value for that feeding event.

#### *Electromyography of the projector muscle*

Electromyographic (EMG) recordings and high-speed video recordings were made from one of the bilaterally paired tongue projector muscles (m. subarcualis rectus, SAR) in three individuals of *Bolitoglossa dofleini* while they fed on crickets.

The morphology of the feeding system of plethodontid salamanders and the EMG methods used here are discussed in a previous paper (Deban and Dicke, 2004) and are reviewed here only briefly. During tongue projection, the elongated tongue skeleton folds medially, becoming a compact projectile as it is pulled and squeezed forward relative to the ceratohyals by the paired SAR muscles. The posterior portion of the SAR (SARP) encompasses the elongated epibranchial cartilages and is in series with the anterior portion (SARA) that inserts on the

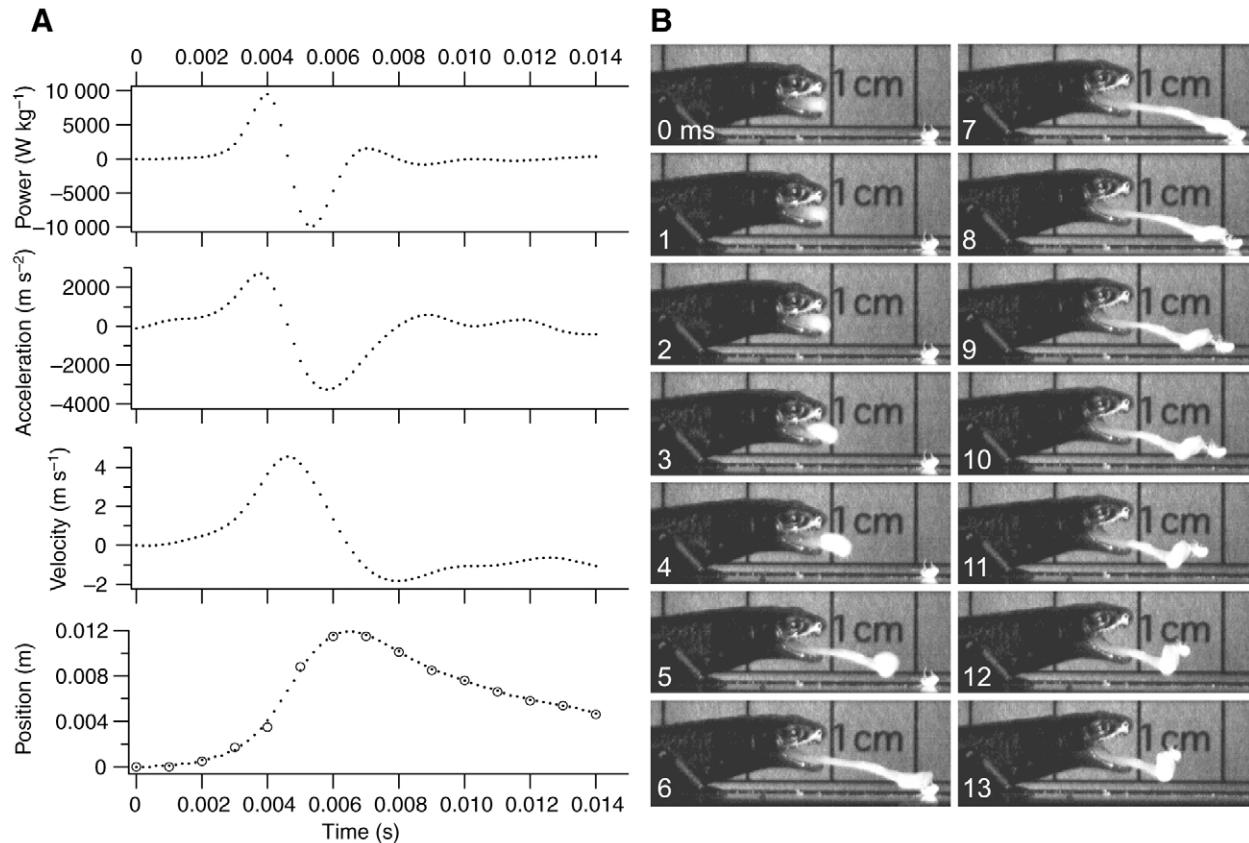


Fig. 2. (A) Kinematic profiles from a representative feeding of extremely high power in *Bolitoglossa dofleini* showing required instantaneous muscle-mass-specific power *versus* time in the upper trace, and instantaneous acceleration, velocity, and smoothed and interpolated position *versus* time in the lower traces. Open circles in the position trace indicate raw position data, which correspond exactly to the video frames shown in B. (B) Images of the same feeding. Note the extremely high-power values, and that peak power is achieved early in tongue projection. Times (ms) are from the start of tongue projection.

ceratohyal cartilages in the floor of the mouth. In the species examined here, the tongue skeleton is free from the SAR muscles and can be projected completely from the mouth in a ballistic fashion. It is attached to the body of the salamander by a bundle of tissue that includes the retractor muscles (i.e. the rectus cervicis, RC), blood vessels, nerves and a connective tissue sheath. After the tongue is fully projected, it is withdrawn into the body by the RC muscles, which originate on the pelvis and insert into the tongue pad. These lengthy muscles are slack and even pleated when the tongue is at rest in the mouth (Lombard and Wake, 1977; Deban et al., 1997).

Electrodes were implanted through three or four small incisions in the skin, at the surface of the muscles. An electrode was placed against the anterior portion of the SAR in two individuals through an incision in the skin of the throat.

Formvar-coated nichrome wire was used to construct bipolar patch electrodes. Prior to electrode implantation, salamanders were anesthetized by immersion in a buffered 2% aqueous solution of MS-222 (3-aminobenzoic acid ethyl ester; Sigma, St Louis, MO, USA) for 10–30 min. Electrodes were implanted through a small incision in the skin onto the surface of the right SAR muscle midway along its length. Electrode leads were

glued together with modeling glue and attached to the skin of the back with suture. The ends of the leads were soldered to metal connectors, which were plugged into the probe of the amplifier (Deban and Dicke, 1999).

Salamanders fed readily after recovery from anesthesia, which typically took less than 30 min. Recordings were made within 3 days of recovery, after which electrode positions and spacing were confirmed surgically. A total of 25 feedings from three individuals were recorded. Electromyographic signals were amplified 2000 times by a Grass P511 (West Warwick, RI, USA) differential amplifier. Signals were recorded at a rate of 2000 samples  $\text{s}^{-1}$  on an Apple (Cupertino, CA, USA) Macintosh PowerPC G3 using a National Instruments (Austin, TX, USA) PCI-6034E analog-to-digital card and a custom LabVIEW program. The raw signals were rectified and filtered in LabVIEW to remove 60 Hz line noise, other noise, and low-frequency movement artifacts (Deban and Dicke, 2004).

EMG and video recordings of feedings were made while salamanders stood in a thin layer of water connected to ground in a transparent plastic box, with the retro-reflective material beneath the box. Live crickets were dropped on the

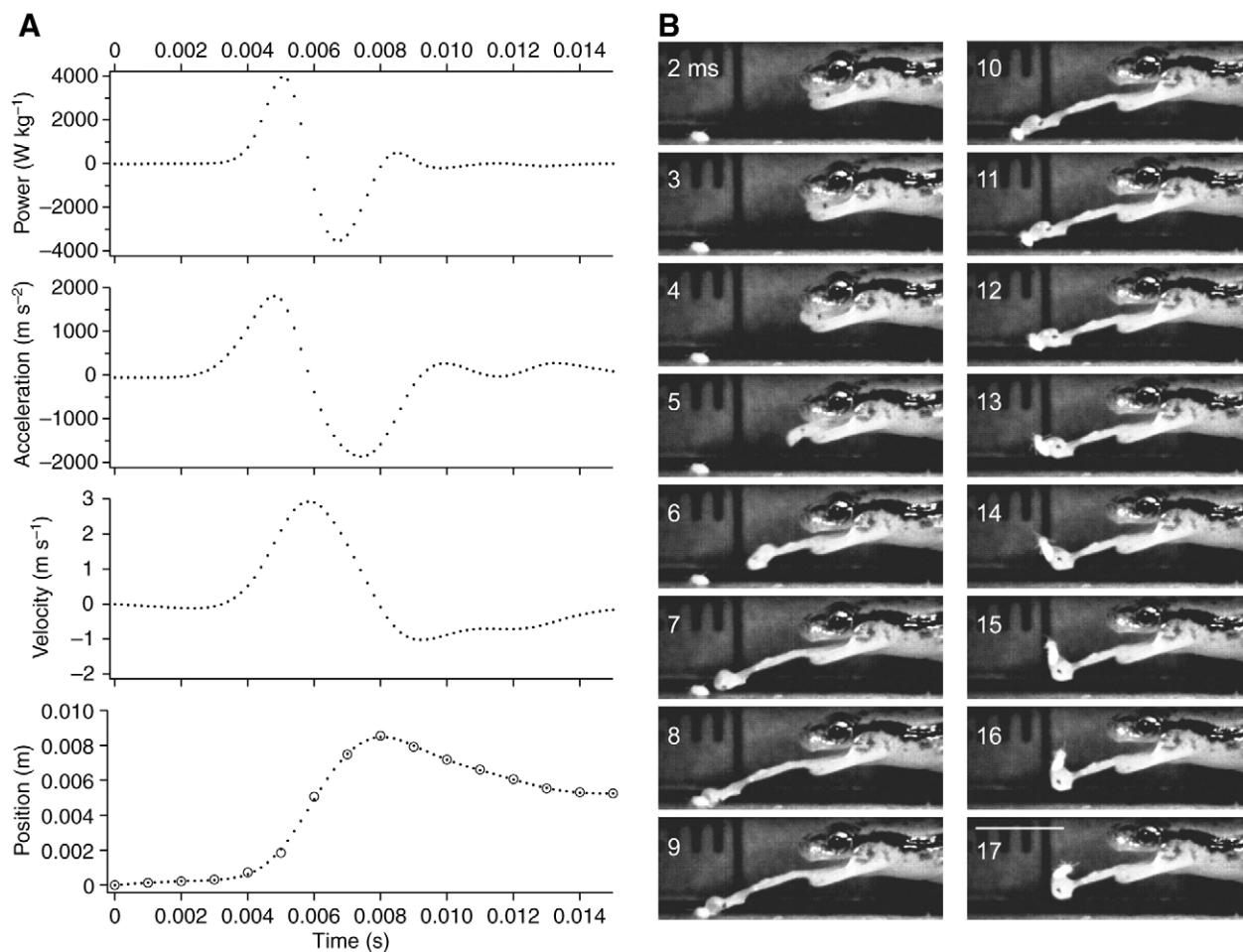


Fig. 3. (A) Kinematic profiles from a representative feeding in *Eurycea guttolineata* showing required instantaneous muscle-mass-specific power *versus* time in the upper trace, and instantaneous acceleration, velocity, and smoothed and interpolated position *versus* time in the lower traces. Open circles in the position trace indicate raw position data, which correspond exactly to the video frames shown in B. (B) Image sequence of the same feeding. Scale bar, 5 mm; times (ms) are from the start of tongue projection.

substrate in front of the salamander to induce feeding. The trigger output on the video camera was connected to a separate channel on the data acquisition card, allowing synchronization of the EMG signals and the videos to within one video frame (1–2 ms).

#### *Analysis of electromyograms*

Five measurements were made from the rectified EMG burst associated with each prey-capture strike: (1) time of the onset of activity, the time after which activity exceeded background noise levels by twofold for at least 10 ms; (2) time of the offset of activity, the time after which activity dropped below two times background noise levels for at least 10 ms; (3) burst area, the area under the rectified EMG burst (in units of mV s) between times 1 and 2; (4) duration of activity, the onset time minus the offset time, and (5) peak amplitude, the rectified EMG area (in units of mV s) of the 10 ms period of the burst in which this value was maximal.

For each prey-capture strike, the SAR activation-

projection delay was calculated by subtracting the SAR EMG onset time (1 above) from the time of the first appearance of the tongue at the mouth (taken from the synchronized video sequence).

The SAR activation–projection delay corresponds roughly to the duration of time that is available for any elastic structures that are in series with contractile elements to be loaded with potential energy. This loading period was used to estimate the average muscle-mass-specific power that would have to be generated by the projector muscles for each feeding attempt, the average muscle-mass-specific power input, by taking the average muscle-mass-specific power output and multiplying it by the ratio of unloading period duration (i.e. time to maximum velocity) to loading period duration. The loading duration includes the unknown time required after activation for the projector muscle to develop tension (i.e. the ‘electromechanical delay’).

To examine the relationship between projector muscle activation and tongue projection kinematics, four analyses of

Table 1. Summary statistics of ten kinematic variables for each genus of salamander

	Mean	s.e.m.	<i>N</i>	Minimum	Maximum
<i>Bolitoglossa</i>					
Maximum tongue reach (m)	0.015	0.001	57	0.003	0.032
Maximum relative tongue reach (%)	0.166	0.008	57	0.038	0.314
Maximum velocity (m s <sup>-1</sup> )	3.892	0.145	57	1.573	7.032
Maximum acceleration (m s <sup>-2</sup> )	1740	109	57	619	4492
Maximum specific power (W kg <sup>-1</sup> )	4109	424	57	711	18129
Total specific work (J kg <sup>-1</sup> )	6.4	0.5	57	0.9	19.5
Time of maximum tongue reach (s)	0.007	0.0004	57	0.003	0.013
Time of maximum velocity (s)	0.004	0.0003	57	0.002	0.011
Time of maximum acceleration (s)	0.003	0.0004	57	0.0004	0.025
Time of maximum specific power (s)	0.003	0.0002	57	0.001	0.009
<i>Eurycea</i>					
Maximum tongue reach (m)	0.009	0.001	20	0.005	0.016
Maximum relative tongue reach (%)	0.234	0.012	20	0.113	0.334
Maximum velocity (m s <sup>-1</sup> )	2.477	0.111	20	1.267	3.174
Maximum acceleration (m s <sup>-2</sup> )	1172	95	20	473	1992
Maximum specific power (W kg <sup>-1</sup> )	2818	322	20	552	5921
Total specific work (J kg <sup>-1</sup> )	4.1	0.3	20	1.0	6.5
Time of maximum tongue reach (s)	0.007	0.0004	20	0.004	0.011
Time of maximum velocity (s)	0.004	0.0003	20	0.002	0.007
Time of maximum acceleration (s)	0.002	0.0002	20	0.002	0.005
Time of maximum specific power (s)	0.003	0.0002	20	0.002	0.005
<i>Hydromantes</i>					
Maximum tongue reach (m)	0.027	0.002	18	0.012	0.040
Maximum relative tongue reach (%)	0.420	0.030	18	0.191	0.639
Maximum velocity (m s <sup>-1</sup> )	3.410	0.235	18	1.935	4.868
Maximum acceleration (m s <sup>-2</sup> )	623	78	18	220	1174
Maximum specific power (W kg <sup>-1</sup> )	1860	330	18	273	4305
Total specific work (J kg <sup>-1</sup> )	6.5	0.9	18	1.8	12.3
Time of maximum tongue reach (s)	0.013	0.001	18	0.008	0.019
Time of maximum velocity (s)	0.009	0.001	18	0.003	0.015
Time of maximum acceleration (s)	0.006	0.001	18	0.000	0.011
Time of maximum specific power (s)	0.007	0.001	18	0.001	0.012

covariance (ANCOVAs) were performed with individual as the effect and one of four EMG variables as the covariate: SAR activation–projection delay, SAR EMG burst duration, SAR EMG burst area, and SAR EMG peak amplitude. The ANCOVAs examined the effects of individual and each of these four EMG variables on nine kinematic variables: maximum velocity, maximum tongue reach, maximum acceleration, maximum muscle-mass-specific power, muscle-mass-specific work, time of maximum tongue reach, time of maximum velocity, time of maximum acceleration and time of maximum power output. The inclusion of an individual term in the model accounted for the influence of individual variation, both biological variation and electrode variation. Individual variation was present in a few variables, but will not be discussed. The individual  $\times$  covariate interaction was not significant for any variable in any of the four analyses, so it was dropped from the model to improve statistical power. These analyses were performed using StatView 5.0 for Macintosh.

Least-squares regressions and coefficients of determination

( $r^2$ ) were calculated for variables that showed a significant effect in the ANCOVAs, to examine the relationship between EMG and kinematic variables.

## Results

Prey capture in all species consisted of orientation of the salamander toward the prey followed by rapid protraction and retraction of the tongue. Prey adhered to the sticky tongue pad and were drawn into the mouth by the retracting tongue (Figs 1–3). Prey were captured at a range of distances in each species, with *Hydromantes* (Fig. 1) species capturing prey from the greatest distances (12–40 mm) followed by *Bolitoglossa* (3–32 mm; Fig. 2) and *Eurycea* species (4–11 mm; Fig. 3). *Hydromantes* also displayed the greatest relative maximum tongue reach (19–64% SVL), and *Eurycea* (11–33% SVL) showed a slightly greater relative maximum tongue reach than *Bolitoglossa* (4–31% SVL).

Duration of tongue protraction (i.e. time to maximum tongue reach) was less than 20 ms in all feedings of all species, and

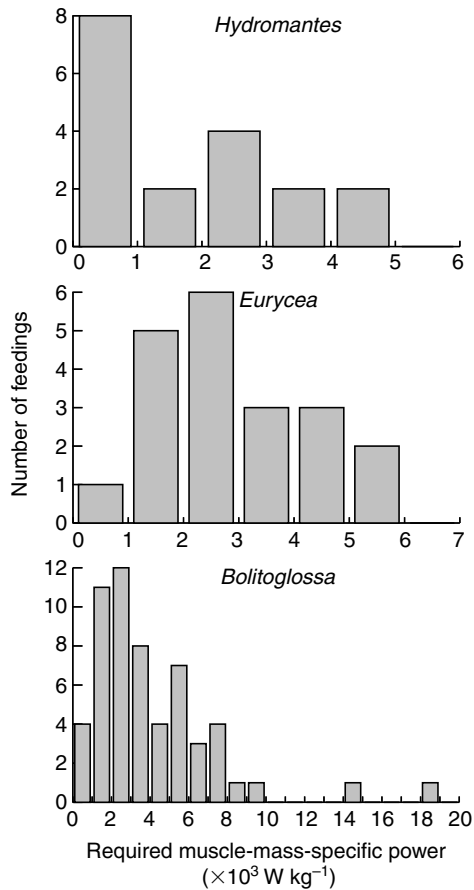


Fig. 4. Frequency histograms of all feedings from *Hydromantes*, *Eurycea* and *Bolitoglossa*, showing number of feedings analyzed with different levels of required muscle-mass-specific power. In all taxa, most feedings are over  $1000 \text{ W kg}^{-1}$ , and extremely high power was observed repeatedly, but less frequently.

the greatest in *Hydromantes* (8–19 ms), followed by *Bolitoglossa* (3–13 ms) and *Eurycea* (4–11 ms) (Table 1).

#### Tongue projection kinematics

Maximum velocities and accelerations of the tongue during projection were high, in accordance with the brief duration of the movement (Table 1). Average maximum velocities were highest in *Hydromantes genei* ( $4.6 \pm 0.1 \text{ m s}^{-1}$ , maximum  $4.9 \text{ m s}^{-1}$ , means  $\pm$  s.e.m.), followed by *H. imperialis* ( $4.0 \pm 0.0 \text{ m s}^{-1}$ , maximum  $4.2 \text{ m s}^{-1}$ ), *Bolitoglossa* ( $3.8 \pm 0.1 \text{ m s}^{-1}$ , maximum  $7.0 \text{ m s}^{-1}$ ), *H. platycephalus* ( $2.7 \pm 0.2 \text{ m s}^{-1}$ , maximum  $3.7 \text{ m s}^{-1}$ ), *Eurycea wilderae* ( $2.5 \pm 0.1 \text{ m s}^{-1}$ , maximum  $3.1 \text{ m s}^{-1}$ ) and *E. guttolineata* ( $2.3 \pm 0.2 \text{ m s}^{-1}$ , maximum  $2.7 \text{ m s}^{-1}$ ).

Average maximum accelerations were highest in *Bolitoglossa* ( $1740 \pm 109 \text{ m s}^{-2}$ , maximum  $4492 \text{ m s}^{-2}$ ), followed by *Eurycea wilderae* ( $1377 \pm 104 \text{ m s}^{-2}$ , maximum  $1992 \text{ m s}^{-2}$ ), *H. genei* ( $1009 \pm 58 \text{ m s}^{-2}$ , maximum  $1174 \text{ m s}^{-2}$ ), *H. imperialis* ( $810 \pm 108 \text{ m s}^{-2}$ , maximum  $918 \text{ m s}^{-2}$ ), *E. guttolineata* ( $792 \pm 64 \text{ m s}^{-2}$ , maximum  $1039 \text{ m s}^{-2}$ ) and *H. platycephalus* ( $413 \pm 65 \text{ m s}^{-2}$ , maximum  $984 \text{ m s}^{-2}$ ).

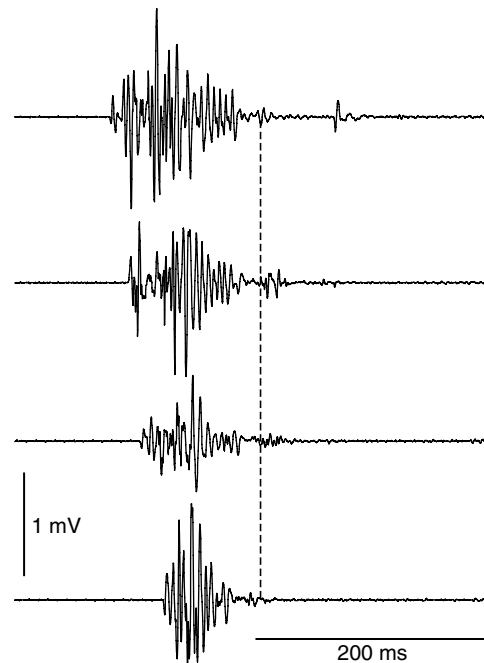


Fig. 5. Electromyographs from the subarcualis rectus muscle in four feedings of one individual of *Bolitoglossa dofleini*. Traces are aligned at the time that the tongue first appears at the mouth, marked by the vertical broken line. Note that EMG activity has nearly ceased by this time and that considerable modulation occurs in the duration and timing of the EMG burst.

All six species achieved maximum required muscle-mass-specific instantaneous power output above  $2000 \text{ W kg}^{-1}$  in at least one feeding (Table 1). (All required muscle-mass-specific power values and work values are reported as  $\text{W kg}^{-1}$  SAR muscle or  $\text{J kg}^{-1}$  SAR muscle, not  $\text{kg}^{-1}$  body mass.) *Bolitoglossa dofleini* achieved the highest maximum required muscle-mass-specific power at  $18\,129 \text{ W kg}^{-1}$ , followed by *Eurycea wilderae* ( $5921 \text{ W kg}^{-1}$ ), *Hydromantes genei* ( $4305 \text{ W kg}^{-1}$ ), *H. imperialis* ( $2923 \text{ W kg}^{-1}$ ), *E. guttolineata* ( $2467 \text{ W kg}^{-1}$ ) and *H. platycephalus* ( $2443 \text{ W kg}^{-1}$ ) (Fig. 4). Average maximum required power values of all feedings for each species also exceeded the expected value of  $1121 \text{ W kg}^{-1}$  (Table 1): *B. dofleini* achieved  $4109 \pm 424 \text{ W kg}^{-1}$ , followed by *H. genei* ( $3700 \pm 273 \text{ W kg}^{-1}$ ), *E. wilderae* ( $3377 \pm 405 \text{ W kg}^{-1}$ ), *H. imperialis* ( $2495 \pm 428 \text{ W kg}^{-1}$ ), *E. guttolineata* ( $1778 \pm 229 \text{ W kg}^{-1}$ ) and *H. platycephalus* ( $908 \pm 186 \text{ W kg}^{-1}$ ).

Total muscle-mass-specific work performed during tongue projection ranged from 0.9 to  $19.5 \text{ J kg}^{-1}$ , averaging  $6.3 \pm 1.2 \text{ J kg}^{-1}$ . *H. genei* performed the most average muscle-mass-specific work at  $11.2 \text{ J kg}^{-1}$  and *E. guttolineata* the lowest at  $3.7 \text{ J kg}^{-1}$  (Table 1).

#### Projector muscle activation

The EMG recordings from *Bolitoglossa dofleini* reveal that the SAR muscle (i.e. tongue projector muscle) began activity 0.082–0.213 s before the tongue leaves the mouth. This SAR

Table 2. Results of ANCOVA showing effects of SAR activity–projection delay, SAR EMG area and SAR EMG duration on nine kinematic variables in three individuals of *Bolitoglossa dofleini*

Variables	SAR activity–projection delay		EMG area		EMG duration	
	F	P	F	P	F	P
Maximum tongue reach	4.618	0.0441*	4.679	0.0428*	2.183	0.1551
Maximum tongue velocity	16.235	<b>0.0008*</b>	5.424	0.0305*	2.328	0.1427
Maximum tongue acceleration	0.096	0.76	0.58	0.4551	0.0001	0.9908
Maximum specific power output	1.722	0.2043	1.343	0.2601	1.679	0.2098
Total specific work	5.954	0.0241*	4.682	0.0428*	2.191	0.1544
Time of maximum tongue reach	1.299	0.2679	1.234	0.2779	1.415	0.2482
Time of maximum velocity	5.413	0.0306*	1.141	0.2982	3.667	0.0699
Time of maximum acceleration	0.1680	0.6864	0.626	0.4393	3.080	0.0946
Time of maximum power output	4.887	0.0389*	0.925	0.3476	4.249	0.0525

Degrees of freedom are 1 and 20.

SAR, m. subarcualis rectus muscle.

\*Significant effect at  $P=0.05$  level. Bold indicates significant effect at Bonferroni adjusted  $\alpha=0.0056$ .

activation–projection delay averages  $0.117\pm 0.005$  s (mean  $\pm$  s.e.m.) (Fig. 5). SAR EMG burst duration averages  $0.171\pm 0.012$  s (from 0.073 to 0.282 s), burst area averages  $12.4\pm 0.7$  mV s (from 5.1 to 20.2 mV s), and peak amplitude averages  $0.71\pm 0.04$  mV (from 0.271 to 1.144 mV).

The average power estimated to have been generated by the SAR during the 0.117 s loading period (the average muscle-mass-specific power input) ranged from 10 to 167 W kg<sup>-1</sup> and averaged  $54\pm 4$  W kg<sup>-1</sup>.

Both SAR activation–projection delay and SAR EMG area had a significant, positive, effect on maximum tongue reach, maximum tongue velocity, and total muscle-mass-specific work, as shown by the ANCOVA (Table 2). SAR activation–projection delay additionally had a significant, positive effect on the time of maximum velocity and the time of maximum power output. There was no significant effect of EMG duration or EMG peak amplitude on any of the kinematic variables. Maximum muscle-mass-specific power output was not significantly affected by any of the EMG variables. SAR activation–projection delay showed a coefficient of determination ( $r^2$ ) of 0.22 with maximum tongue reach, 0.26 with maximum tongue velocity, 0.24 with total muscle-mass-specific work, 0.22 with time of maximum velocity, and 0.21 with time of maximum power output (Fig. 6). SAR EMG area has an  $r^2$  of 0.21 with maximum tongue reach, 0.22 with total muscle-mass-specific work, and 0.24 with maximum velocity (Fig. 7).

## Discussion

### Feeding behavior and tongue projection

The tongue projection behavior in the *Hydromantes* examined in this study is consistent with previous descriptions (Deban et al., 1997; Deban and Dicke, 1999; Deban and Dicke, 2004). The *Bolitoglossa* and *Eurycea* displayed tongue projection of shorter duration than *Hydromantes*; however, these species did not project their tongues to as great distance as *Hydromantes*, in

neither absolute nor relative terms. This results are in accord with predictions based on the morphology of the tongue apparatus, namely that the length of the folded tongue skeleton (particularly the epibranchials) is greatest in *Hydromantes* (Lombard and Wake, 1976; Lombard and Wake, 1977).

The duration of tongue projection in all these species is very brief when compared to published values from other salamander taxa. The brief tongue projection durations are no doubt related to the ballistic mode of tongue projection, in which high velocities must be achieved to propel the tongue to the target under its own momentum. Among other salamanders in the family Plethodontidae that lack ballistic projection, some take about the same time to protract the tongue as *Hydromantes* ( $13\pm 1$  ms), but all take longer than *Eurycea* and *Bolitoglossa* (both  $7\pm 0.04$  ms): *Ensatina eschscholtzii* protracts the tongue fully in an average of 15 ms (Deban, 1997a), *Pseudotriton ruber* requires 11 ms (Deban, 1997b), *Plethodon glutinosus* takes 19 ms, and *Desmognathus quadramaculatus* takes 37 ms (Larsen, Jr et al., 1989). Salamanders from other families, none of which have free tongue pads or ballistic projection, require still longer: *Ambystoma mabeei* takes 16 ms, *A. cingulatum* takes 87 ms (Beneski, Jr et al., 1995), *Ambystoma tigrinum* 40 ms (Dockx and de Vree, 1986), *Salamandra salamandra* 22–84 ms (Dockx and de Vree, 1986; Miller and Larsen, Jr, 1990), *Paramesotriton hongkongensis* 112 ms (Miller and Larsen, 1990); *Taricha torosa* 80–140 ms (Findeis and Bemis, 1990), *Hynobius kimurae* 25 ms and *H. nebulosus* 36 ms (Larsen et al., 1996).

The distance of tongue protraction also varies widely among salamanders (Wake and Deban, 2000). *Hydromantes*, *Eurycea* and *Bolitoglossa* (and all other bolitoglossines) possess enhanced tongue projection abilities, in both brevity and reach. Their maximum tongue projection distances range from 31 to 64% of SVL and 16 to 40 mm (Table 1). In comparison, *Ambystoma californiense* can protract its tongue 2.4 mm beyond the jaw tips and *A. mabeei* only 0.3 mm (Beneski, Jr et al., 1995); *Salamandrella keyserlingii* protracts its tongue

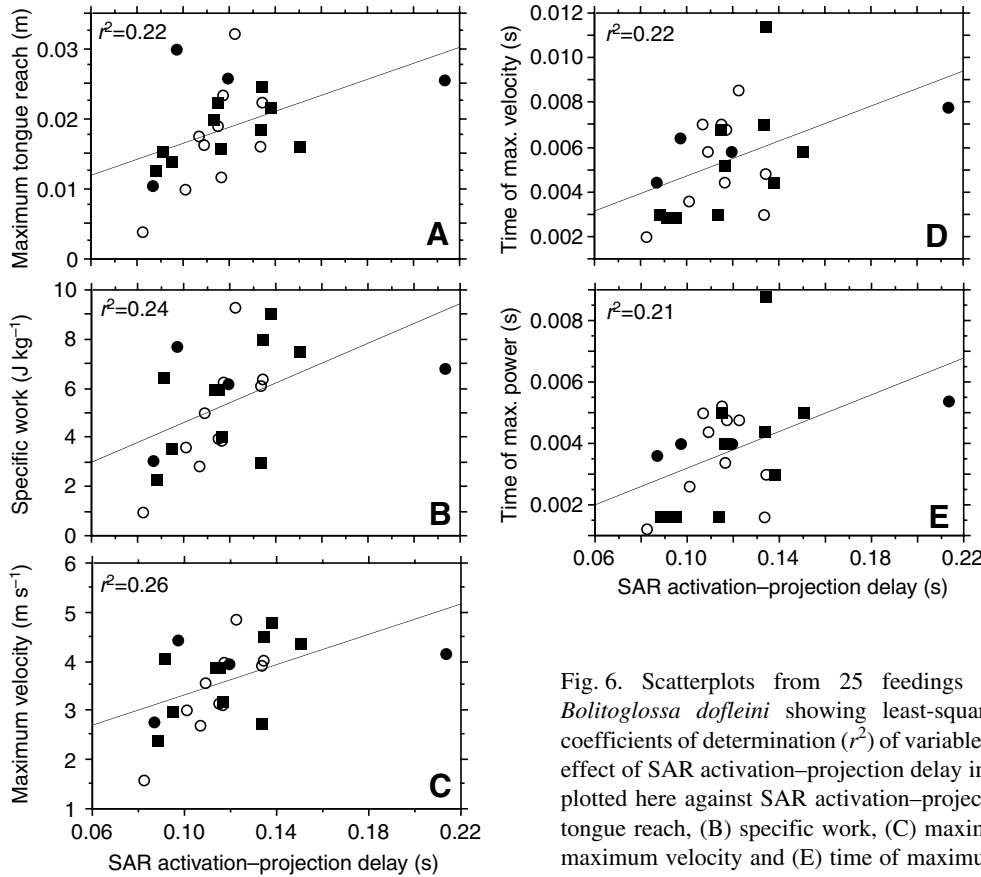


Fig. 6. Scatterplots from 25 feedings in three individuals of *Bolitoglossa dofeini* showing least-squares regression lines and coefficients of determination ( $r^2$ ) of variables that showed a significant effect of SAR activation-projection delay in the ANCOVA (see text), plotted here against SAR activation-projection delay: (A) maximum tongue reach, (B) specific work, (C) maximum velocity, (D) time of maximum velocity and (E) time of maximum power.

6.6 mm (Wake and Deban, 2000), *Tylotriton verrucosus* 2.7 mm, and *Salamandrina terdigitata* 7.4 mm (Miller and Larsen, Jr, 1990). Relative tongue reach distances reported are 7% of SVL for the plethodontids *Desmognathus quadramaculatus* and *Plethodon jordani*, and 15% in *Ensatina eschscholtzii* (Wake and Deban, 2000). Among those taxa previously studied with ballistic tongue projection, *Bolitoglossa occidentalis* projects its tongue up to 17 mm or 44% of SVL (Thexton et al., 1977; Larsen, Jr et al., 1989), *Bolitoglossa subpalmata* has been recorded reaching 30 mm, and *Hydromantes italicus* 50 mm (Roth, 1976), and the greatest tongue reach occurs in *Hydromantes supramontis*, which has been recorded projecting its tongue 60 mm or 80% of SVL (Deban et al., 1997).

Maximum tongue projection velocities and accelerations have not been published for other salamander species, but they have been measured in the chameleon, another ballistic-tongued animal. *Chameleo pardalis* and *C. melleri* produce peak accelerations of the tongue pad of  $340\text{--}374 \text{ m s}^{-2}$ , and a peak velocity of  $6 \text{ m s}^{-1}$  (de Groot and van Leeuwen, 2004), and *Chameleo oustaleti* achieves a peak acceleration of  $490 \text{ m s}^{-2}$  (Wainwright et al., 1991). The velocity is higher than the highest velocity achieved by the salamanders ( $4.6 \text{ m s}^{-1}$  in *Hydromantes*), but the chameleon's accelerations are much lower (compared to  $413\text{--}1740 \text{ m s}^{-2}$  in the salamanders). This makes sense when we consider that the chameleons that have been studied are much larger animals, have a longer 'track' on

which to accelerate the tongue to a given velocity, compared to the salamanders, and shoot their tongues a greater absolute and relative distance. A similar pattern emerges from the comparison of values among the salamander species of this study. *Hydromantes* have the longest epibranchials and projector muscles, by far, with which to accelerate the tongue. Two of the *Hydromantes* have the lowest accelerations, two have greater velocity, and all have greater tongue reach than the other taxa.

The total mass-specific work performed by the salamander tongue projector muscles (maxima are  $5\text{--}20 \text{ J kg}^{-1}$ ; Table 1) is at the lower end of the range of values obtained from other vertebrate musculoskeletal systems, suggesting that the muscles may be working, on average, at low strain and/or low stress. Work is estimated at  $28 \text{ J kg}^{-1}$  in *Chameleo* [ $56 \text{ mJ } 2 \text{ g}^{-1}$  (de Groot and van Leeuwen, 2004)]. In the pectoralis muscles of various birds of different sizes, work ranged from 16 to  $56 \text{ J kg}^{-1}$ , with the larger values achieved by the larger birds (Askew et al., 2001). Limb muscles of jumping bullfrogs averaged  $27 \text{ J kg}^{-1}$  (with a strain of 26% in one muscle) (Olson and Marsh, 1998). In mouse soleus muscles, work was measured at  $4.5\text{--}15.5 \text{ J kg}^{-1}$  with *in vitro* work loop experiments with strains ranging from 6–11% of resting muscle length (the highest work corresponded to the highest strain) (Askew and Marsh, 1997). One estimate of maximum work for skeletal muscle is  $57\text{--}113 \text{ J kg}^{-1}$ , given a maximum stress of  $200\text{--}400 \text{ kPa}$  ( $\text{kN m}^{-2}$ ) and a strain of 30% (Pennycuik, 1992).

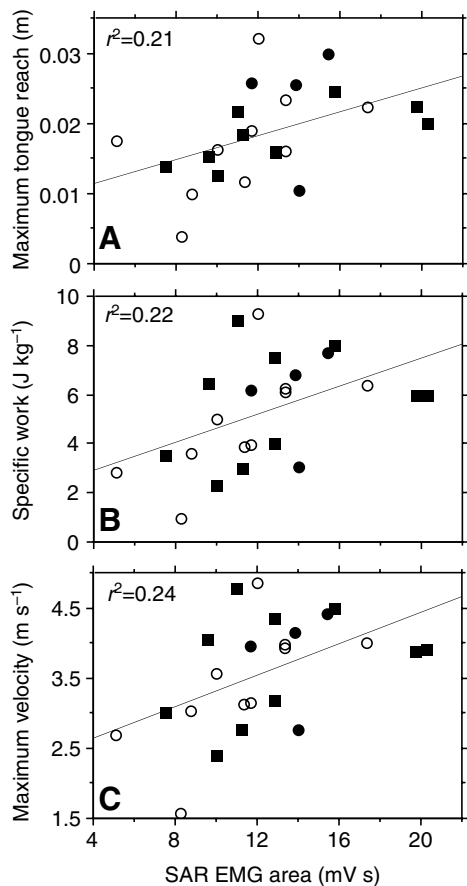


Fig. 7. Scatterplots from 25 feedings in three individuals of *Bolitoglossa dofleini* showing least-squares regression lines and coefficients of determination ( $r^2$ ) of variables that showed a significant effect of SAR EMG area in the ANCOVA, plotted against SAR EMG area: (A) maximum tongue reach, (B) specific work and (C) maximum velocity.

However, when work is computed as the area under the curve of isometric tension plotted against length, values as high as  $220 \text{ J kg}^{-1}$  (for frog striated muscle) are estimated (Alexander and Bennet-Clark, 1977). If we assume that the tongue projector muscles of salamanders are maximally recruited, the calculated work values suggest that the muscles spend little or no time near the portion of their length–tension curves where high stress is developed, or they operate at low strains, or both.

#### Required muscle power output

Instantaneous required mass-specific power output of the tongue projector muscle, the SAR, in the salamanders studied here is extremely high ( $2443\text{--}18129 \text{ W kg}^{-1}$ ) when compared to other muscular systems that have been studied, both episodically and cyclically contracting muscles. Among episodic systems, the semimembranosus muscle of *Rana pipiens*, when used in maximal jumping, reached  $373 \text{ W kg}^{-1}$ , as shown by *in vitro* contractile experiments (Lutz and Rome, 1996). The jumping musculature in hyloid frogs was estimated from kinematics of high-speed movies to produce an average

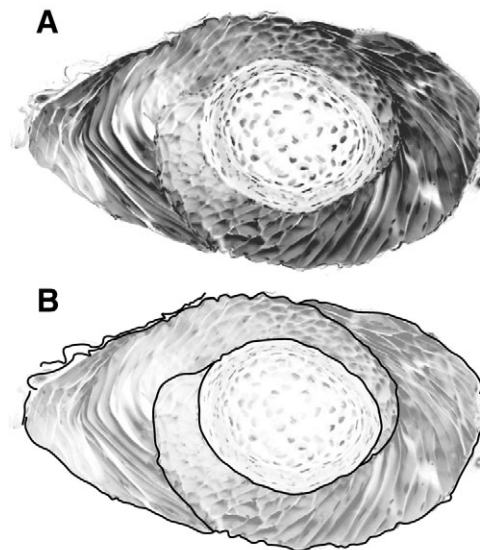


Fig. 8. (A) Confocal laser microscope image of a cross section of the tongue projector muscle (m. subarcualis rectus) of *Hydromantes genei*. The epibranchial cartilage is in the center, surrounded by short ( $\sim 1 \text{ mm}$ ) muscle fibers with a variety of orientations. (B) The same image with the position of the collagenous aponeuroses marked as black lines. All muscle fibers originate and insert on these aponeuroses. The section is approximately  $2 \text{ mm}$  in its widest diameter.

required muscle-mass-specific power of  $500 \text{ W kg}^{-1}$  (Marsh and John-Alder, 1994), and a peak instantaneous muscle-mass-specific power that is probably twice that,  $1000 \text{ W kg}^{-1}$ . An even higher value was estimated for the hind limb muscles of the bushbaby, *Galago senegalensis*, which achieved  $2350 \text{ W kg}^{-1}$  (Bennet-Clark, 1976), a figure confirmed by *in vivo* inverse dynamics analysis (Aerts, 1998). The tongue projector muscle of the chameleon achieves  $2340\text{--}3168 \text{ W kg}^{-1}$  for required muscle-mass-specific power output (de Groot and van Leeuwen, 2004), and the jaw depressor muscles of the toad *Bufo* achieve the highest value yet,  $9600 \text{ W kg}^{-1}$  during ballistic mouth opening (Lappin et al., 2006).

Cyclical locomotor systems for which power has been estimated or measured also show values lower than the SAR of the ballistic-tongued salamanders. Hummingbird flight muscles produce  $100 \text{ W kg}^{-1}$  (Wells and Ellington, 1994), mouse extensor digitorum longus muscles achieve  $372 \text{ W kg}^{-1}$  in *in vitro* maximum isotonic power (Askew and Marsh, 1997), and the iliofibularis muscles of the lizard *Dipsosaurus dorsalis* which are used in acceleration, achieved  $460 \text{ W kg}^{-1}$  at  $40^\circ\text{C}$ , measured *in vitro* (Marsh and Bennett, 1985). Based on the breaking strength of the muscle tendons, the pectoralis of the pigeon is estimated at  $860 \text{ W kg}^{-1}$  maximum (Pennycuick and Parker, 1966), and based on *in vitro* work loop experiments, that of the quail achieves  $1121 \text{ W kg}^{-1}$  (Askew and Marsh, 2001). A similar value was estimated for accelerating lizards of the genus *Acanthodactylus*:  $952 \text{ W kg}^{-1}$  *in vitro* and  $940 \text{ W kg}^{-1}$  *in vivo* (Curtin et al., 2005).

In any musculoskeletal system in which connective tissue is in series with a muscle, the work of the muscle is redistributed temporally to some extent due to compliance of the connective tissue (Alexander, 2002). In certain cases, this redistribution can result in very high rates of energy release (i.e. power output) because some tissues, such as collagen, are stiffly elastic and can store strain energy and then release that energy faster than the contractile elements of muscle. Maximizing power output is critical for performance of ballistic movements such as throwing, tongue projection and jumping, because these movements require high kinetic energy to be achieved within a limited excursion (Alexander, 1968; Olson and Marsh, 1998; Alexander, 2002). Although a small amount of elastic strain energy can be stored in muscle tissue (Alexander and Bennet-Clark, 1977), in many systems with power enhancement, such as jumping in frogs, fleas and locusts, and punching in stomatopods, the energy is stored in connective tissues outside the muscle tissue (Bennet-Clark and Lucey, 1967; Bennet-Clark, 1975; Peplowski and Marsh, 1997; Olson and Marsh, 1998; Patek et al., 2004).

Examples of the storage of strain energy that results in increased power production in vertebrates include tongue projection in chameleons and toads, jumping in bushbabies, and accelerating in turkeys. In the chameleon, the work of the accelerator muscle of the tongue is redistributed temporally by elastic structures in the tongue. This set of nested connective tissue sheaths surrounds the tongue skeleton and strain longitudinally when the accelerator muscle contracts. As they slide off the end of the tongue skeleton the sheaths recoil radially and help to accelerate the tongue pad (de Groot and van Leeuwen, 2004). In toads, elastic structures at both the origin and insertion of the depressor mandibulae muscle as well as within the muscle itself have been demonstrated to recoil during the fast mouth opening that powers tongue projection (Lappin et al., 2006). Elastic storage also occurs in the hindlimbs of accelerating, running turkeys, which achieve peak muscle-mass-specific power outputs over  $400 \text{ W kg}^{-1}$  (Roberts and Scales, 2002). The system is thought to achieve this high-power output *via* a mechanism in which tendons in series with extensor muscles store energy during the first half of stance and then release energy and propel the bird during the second half of stance. In the bushbaby, the aponeuroses within the vastus muscle-tendon complex get stretched during the pre-jump crouch and during the early part of push-off and recoil later in push-off, to increase the power output of the vastus muscles (Aerts, 1998).

In salamander tongue projection, no elastic, energy-storing structures have been definitively identified, but two lines of evidence suggest that an elastic power enhancer is operating: the high-power output calculated for tongue projection that is discussed above, and the timing of projector muscle activation relative to tongue movements. In *Bolitoglossa* the projector muscle becomes active 82–213 ms (average  $117 \pm 5$  ms) before the tongue appears at the mouth, which is sufficient time for elastic structures to be loaded prior to recoil. The muscle fibers of the SARP are short ( $\sim 1$  mm) and exclusively fast twitch

(Dicke et al., 1995) and, as such, probably reach peak tension within 30 ms of the start of electrical activity, as do other amphibian fast twitch muscles (Luff and Proske, 1979; Lännergren et al., 1982; Lutz and Rome, 1996), and could begin stretching series elastic elements well before that. Aponeuroses lie in series with the muscle fibers in the complex SARP muscle (Fig. 8) and a double-layered collagenous sheath lines the lumen of the muscle, either of which may act as a spring. However, it is not yet known how these structures are loaded during muscle contraction. The SAR activation–projection delay is similar in duration to that of the other ballistic feeding systems with power enhancement: in *Chameleo*, the tongue accelerator muscle is activated 200–300 ms prior to the start of tongue projection (Wainwright and Bennett, 1992; de Groot and van Leeuwen, 2004), and in *Bufo*, EMG activity of the jaw depressor muscles begins 150–250 ms prior to ballistic mouth opening (Lappin et al., 2006).

Also in accord with the hypothesis of a power enhancer are the estimated values of the maximum power that the SAR generates during the hypothesized loading phase of tongue projection. These values ( $17\text{--}436 \text{ W kg}^{-1}$ , average  $129 \pm 11 \text{ W kg}^{-1}$ ) are within the physiological limits for direct power production of other skeletal muscles that have been studied, which have maxima that range from  $174\text{--}1121 \text{ W kg}^{-1}$  (Marsh and Bennett, 1985; Lutz and Rome, 1996; Askew and Marsh, 1997; Williamson et al., 2001; Curtin et al., 2005). The average value of  $129 \text{ W kg}^{-1}$  is comparable to that of *Chameleo*, which is estimated at  $144 \text{ W kg}^{-1}$  (de Groot and van Leeuwen, 2004).

One last piece of evidence that supports the power enhancement model is the relationship between SAR muscle activity and tongue projection kinematics. When a muscle performs work there should be correlations between certain EMG parameters and the amount of work performed. For example, in breathing in alligators, the EMG activity of several ventilatory muscles is positively and significantly correlated with tidal volume (Farmer and Carrier, 2000). In a system in which the muscle applies force through a series elastic element, energy is still conserved and that relationship should persist. In *Hydromantes*, SAR EMG area has been shown to be positively and significantly correlated with maximum tongue reach (Deban and Dicke, 2004). In the *Bolitoglossa* examined here, SAR EMG area is positively and significantly correlated with maximum tongue reach, maximum tongue velocity and total muscle-mass-specific work, as expected (Table 2). However, because elastic elements should essentially uncouple the rate of work production by the muscle (i.e. power input) from the rate of work performed on the tongue skeleton (i.e. power output), which is measurable kinematically, we expect no correlation between SAR EMG area and maximum power output. There is in fact no relationship between SAR EMG area and maximum muscle-mass-specific power output. The timing of muscle activation relative to tongue movements, on the other hand, should show a relationship with kinematic performance measures, because we expect that loading of elastic structures

will take longer in tongue projection episodes of greater effort. SAR activation–projection delay is in fact positively and significantly correlated with several performance measures including maximum tongue reach, maximum velocity, and total muscle-mass-specific work (Table 2). Maximum power production is not correlated with any EMG parameter measured, indicative of an uncoupling of power produced by the muscle and power manifest in the projected tongue.

### Conclusions

The available evidence points to an elastic power enhancer in the ballistic tongue-projection mechanism of plethodontid salamanders, animals which achieve tongue projection distances far greater than other salamanders and project the tongue fully in far less time. This high-power system appears to have evolved concomitantly with ballistic projection in the Plethodontidae, three times independently. Such a system requires three components: a motor to generate mechanical work (i.e. energy), a spring to store the energy, and a latch to control the timing of unloading of the spring. The motor has been identified as the paired subarcualis rectus muscles. What remains to be discovered are the anatomical structures that make up the spring and the latch. In other systems, collagen acts as the spring that stores energy and increases the instantaneous power output of the muscular system, either in the form of tubular sheaths as in the chameleon or aponeuroses as in the bushbaby. In the SARP of *Hydromantes* (Fig. 8), collagen fibers lie in series with the short muscle fibers in the form of aponeuroses as well as a double-layered sheath surrounding the lumen (similar to the situation in chameleons), providing two viable candidates for the spring. The morphology of the SARP of the other species examined here is very similar to that of *Hydromantes*, and likely also contain these collagenous structures. Future work will focus on determining how these structures are loaded prior to tongue projection and how much energy they can store. The latch remains to be identified, but we expect that it is under muscular control to allow elastic elements to be loaded to varying degrees before tongue projection commences, a hypothesis based on the documented ability of these salamanders to precisely modulate their tongue projection distance and velocity (Deban and Dicke, 1999; Deban and Dicke, 2004).

We thank H. Schipper for producing the image of the muscle cross section. J. A. Walker offered helpful advice on smoothing the position data. Kris Lappin and Ulrike Müller provided helpful comments on the manuscript.

### References

- Aerts, P. (1998). Vertical jumping in *Galago senegalensis*: the quest for an obligate mechanical power amplifier. *Philos. Trans. R. Soc. Lond. B Biol. Sci.* **353**, 1607–1620.
- Alexander, R. M. (1968). *Animal Mechanics*. Seattle: University of Washington Press.
- Alexander, R. M. (2002). Tendon elasticity and muscle function. *Comp. Biochem. Physiol.* **133A**, 1001–1011.
- Alexander, R. M. and Bennet-Clark, H. C. (1977). Storage of elastic strain energy in muscle and other tissues. *Nature* **265**, 114–117.
- Askew, G. N. and Marsh, R. L. (1997). The effects of length trajectory on the mechanical power output of mouse skeletal muscles. *J. Exp. Biol.* **200**, 3119–3131.
- Askew, G. N. and Marsh, R. L. (2001). The mechanical power output of the pectoralis muscle of blue-breasted quail (*Coturnix chinensis*): the *in vivo* length cycle and its implications for muscle performance. *J. Exp. Biol.* **204**, 3587–3600.
- Askew, G. N., Marsh, R. L. and Ellington, C. P. (2001). The mechanical power output of the flight muscles of blue-breasted quail (*Coturnix chinensis*) during take-off. *J. Exp. Biol.* **204**, 3601–3619.
- Beneski, J. T., Jr, Larsen, J. H., Jr and Miller, B. T. (1995). Variation in the feeding kinematics of mole salamanders (*Ambystomatidae: Ambystoma*). *Can. J. Zool.* **73**, 353–366.
- Bennet-Clark, H. C. (1975). The energetics of the jump of the locust *Schistocerca gregaria*. *J. Exp. Biol.* **63**, 53–83.
- Bennet-Clark, H. C. (1976). Energy storage in jumping animals. In *Perspectives in Evolutionary Biology* (ed. D. P. Spencer), pp. 467–479. Oxford: Pergamon Press.
- Bennet-Clark, H. C. and Lucey, E. C. (1967). The jump of the flea: a study of the energetics and a model of the mechanism. *J. Exp. Biol.* **47**, 59–67.
- Curtin, N. A., Woledge, R. C. and Aerts, P. (2005). Muscle directly meets the vast power demands in agile lizards. *Proc. Biol. Sci.* **272**, 581–584.
- de Groot, J. H. and van Leeuwen, J. L. (2004). Evidence for an elastic projection mechanism in the chameleon tongue. *Proc. Biol. Sci.* **271**, 761–770.
- Deban, S. M. (1997a). Modulation of prey-capture behavior in the plethodontid salamander *Ensatina eschscholtzii*. *J. Exp. Biol.* **20**, 1951–1964.
- Deban, S. M. (1997b). Development and evolution of feeding behavior and functional morphology in salamanders of the family *Plethodontidae*. PhD thesis, Integrative Biology, University of California, USA.
- Deban, S. M. and Dicke, U. (1999). Motor control of tongue movement during prey capture in plethodontid salamanders. *J. Exp. Biol.* **202**, 3699–3714.
- Deban, S. M. and Dicke, U. (2004). Activation patterns of the tongue-projector muscle during feeding in the imperial cave salamander *Hydromantes imperialis*. *J. Exp. Biol.* **207**, 2071–2081.
- Deban, S. M., Wake, D. B. and Roth, G. (1997). Salamander with a ballistic tongue. *Nature* **389**, 27–28.
- Dicke, U., Mühlenbrock-Lenter, S. and Roth, G. (1995). Fiber types of muscles of the feeding apparatus in plethodontid salamanders. In *Proceedings of the 23rd Göttingen Neurobiology Conference* (ed. N. Elsner and R. Menzel), p. 227. Stuttgart, New York: Georg Thieme.
- Dockx, P. and de Vree, F. (1986). Prey capture and intra-oral food transport in terrestrial salamanders. *Stud. Herpetol.* **1986**, 521–524.
- Farmer, C. G. and Carrier, D. R. (2000). Pelvic aspiration in the American alligator (*Alligator mississippiensis*). *J. Exp. Biol.* **203**, 1679–1687.
- Findeis, E. K. and Bemis, W. E. (1990). Functional morphology of tongue projection in *Taricha torosa* (Urodela: Salamandridae). *Zool. J. Linn. Soc.* **99**, 129–158.
- Lännergren, J., Lindblom, P. and Johansson, B. (1982). Contractile properties of two varieties of twitch muscle fibres in *Xenopus laevis*. *Acta Physiol. Scand.* **114**, 523–535.
- Lappin, A. K., Monroy, J. A., Pilarski, J. Q., Zepnewski, E. D., Pierotti, D. J. and Nishikawa, K. (2006). Storage and recovery of elastic potential energy powers ballistic prey capture in toads. *J. Exp. Biol.* **209**, 2535–2553.
- Larsen, J. H., Jr, Beneski, J. T., Jr and Wake, D. B. (1989). Hyolingual feeding systems of the Plethodontidae: comparative kinematics of prey capture by salamanders with free and attached tongues. *J. Exp. Zool.* **252**, 25–33.
- Larsen, J. H., Beneski, J. T. and Miller, B. T. (1996). Structure and function of the hyolingual system in *Hynobius* and its bearing on the evolution of prey capture in terrestrial salamanders. *J. Morphol.* **227**, 235–248.
- Lombard, R. E. and Wake, D. B. (1976). Tongue evolution in the lungless salamanders, Family Plethodontidae. I. Introduction, theory and general model of dynamics. *J. Morphol.* **148**, 265–286.
- Lombard, R. E. and Wake, D. B. (1977). Tongue evolution in the lungless salamanders, Family Plethodontidae. II. Function and evolutionary diversity. *J. Morphol.* **153**, 39–80.
- Luff, A. R. and Proske, U. (1979). Properties of motor units of the frog iliofibularis muscle. *Am. J. Physiol.* **236**, C35–C40.
- Lutz, G. J. and Rome, L. C. (1996). Muscle function during jumping in frogs. II. Mechanical properties of muscle: implications for system design. *Am. J. Physiol.* **271**, C571–C578.

- Marsh, R. L. and Bennett, A. F.** (1985). Thermal dependence of isotonic contractile properties of skeletal muscle and sprint performance of the lizard *Dipsosaurus dorsalis*. *J. Comp. Physiol. B* **155**, 541-551.
- Marsh, R. L. and John-Alder, H. B.** (1994). Jumping performance of hylid frogs measured with high-speed cine film. *J. Exp. Biol.* **188**, 131-141.
- Miller, B. T. and Larsen, J. H., Jr** (1990). Comparative kinematics of terrestrial prey capture in salamanders and newts (Amphibia: *Urodela: Salamandridae*). *J. Exp. Zool.* **256**, 135-153.
- Olson, J. M. and Marsh, R. L.** (1998). Activation patterns and length changes in hindlimb muscles of the bullfrog *Rana catesbeiana* during jumping. *J. Exp. Biol.* **201**, 2763-2777.
- Patek, S. N., Korff, W. L. and Caldwell, R. L.** (2004). Deadly strike mechanism of a mantis shrimp. *Nature* **428**, 819-820.
- Pennycuik, C. J.** (1992). *Newton Rules Biology: A Physical Approach to Biological Problems*. New York: Oxford University Press.
- Pennycuik, C. J. and Parker, G. A.** (1966). Structural limitations on the power output of the pigeon's flight muscles. *J. Exp. Biol.* **45**, 489-498.
- Peplowski, M. M. and Marsh, R. L.** (1997). Work and power output in the hindlimb muscles of cuban tree frogs *Osteopilus septentrionalis* during jumping. *J. Exp. Biol.* **200**, 2861-2870.
- Roberts, T. J. and Scales, J. A.** (2002). Mechanical power output during running accelerations in wild turkeys. *J. Exp. Biol.* **205**, 1485-1494.
- Roth, G.** (1976). Experimental analysis of prey catching behavior of *Hydromantes italicus* Dunn (Amphibia, Plethodontidae). *J. Comp. Physiol.* **109**, 47-58.
- Thexton, A. J., Wake, D. B. and Wake, M. H.** (1977). Tongue function in the salamander *Bolitoglossa occidentalis*. *Arch. Oral Biol.* **22**, 361-366.
- Wainwright, P. C. and Bennett, A. F.** (1992). The mechanism of tongue projection in chameleons. 1. Electromyographic tests of functional hypotheses. *J. Exp. Biol.* **168**, 1-21.
- Wainwright, P. C., Kraklau, D. M. and Bennett, A. F.** (1991). Kinematics of the tongue projection in *Chamaeleo oustaleti*. *J. Exp. Biol.* **159**, 109-133.
- Wake, D. B. and Deban, S. M.** (2000). Terrestrial feeding in salamanders. In *Feeding: Form, Function and Evolution in Tetrapod Vertebrates* (ed. K. Schwenk), pp. 95-116. San Diego: Academic Press.
- Walker, J. A.** (1997). QuickSAND. Quick smoothing and numerical differentiation for the Power Macintosh.
- Walker, J. A.** (1998). Estimating velocities and accelerations of animal locomotion: a simulation experiment comparing numerical differentiation algorithms. *J. Exp. Biol.* **201**, 981-995.
- Wells, D. J. and Ellington, C. P.** (1994). Beyond the vertebrates: achieving maximum power during flight in insects and hummingbirds. *Adv. Vet. Sci. Comp. Med.* **38**, 219-232.
- Williamson, M. R., Dial, K. P. and Biewener, A. A.** (2001). Pectoralis muscle performance during ascending and slow level flight in mallards (*Anas platyrhynchos*). *J. Exp. Biol.* **204**, 495-507.